

Supporting Information

Influence of Composition Fluctuations on the Linear Viscoelastic Properties of Symmetric Diblock Copolymers near the Order-Disorder Transition

Robert J. Hickey,¹ Timothy M. Gillard,² Timothy P. Lodge,^{1,2} and Frank S. Bates²

¹Department of Chemistry and ²Department of Chemical Engineering and Materials Science,
University of Minnesota, Minneapolis, MN 55455

Rheological Experiments – A Rheometrics Scientific ARES strain-controlled rheometer with the 25 mm diameter parallel plate geometry and a forced convection oven with a nitrogen atmosphere was used for the measurements. PCHE-PE samples ($M_n = 13.6$ kg/mol and 18.9 kg/mol) were loaded to give a gap of approximately 1 mm, heated above any thermal transitions (e.g., glass transitions or order-disorder transitions), cooled at 1 °C/min to specific temperatures (see Tables S1 and S2) and held for 1 hr before running frequency sweeps. Frequency sweeps were run in the frequency range of $0.01 \leq \omega \leq 100$ rad/s. Strains were chosen to maximize torque while remaining in the linear viscoelastic regime.

Small Angle X-ray Scattering (SAXS) – Synchrotron SAXS experiments were conducted at the DND-CAT 5-ID-D beamline at the Advanced Photon Source located in Argonne National Laboratory (Argonne, IL USA) using the triple-detector small-, middle-, and wide-angle X-ray scattering (SAXS/MAXS/WAXS) instrument. An X-ray wavelength of 0.756 Å was used with SAXS and MAXS sample-to-detector distances of approximately 8.5 m and 1 m, respectively. SAXS data were collected with a Rayonix area CCD detectors. All scattering patterns were nearly azimuthally isotropic and were azimuthally integrated to obtain 1D plots of intensity (in arbitrary units) versus scattering wave vector $q = 4\pi\lambda^{-1}\sin(\theta/2)$. The PCHE-PE-14 sample was loaded in a 1.5 mm nominal diameter quartz capillary (Charles Supper Company) and the temperature was controlled during SAXS experiments with a modified Linkam HFS91 hot stage. Prior to the SAXS experiments, the sample was heated above T_{ODT} to equilibrate the sample in the disorder phase in order to remove any processing history, slowly cooled (ca. 1 °C/min) to 140 °C, annealed at 140 °C under vacuum for 15 hrs, and then quenched to room temperature to freeze the equilibrium structure. At the beamline, the sample was quickly reheated to 140 °C to record the equilibrium structure at this temperature. The sample was then heated to 300 °C stopping at several temperatures to collect scattering patterns of the equilibrium structure. The sample was equilibrated at each temperature for approximately 1 min prior to data collection while changes in temperature between measurements were fast (> 20 °C/min).

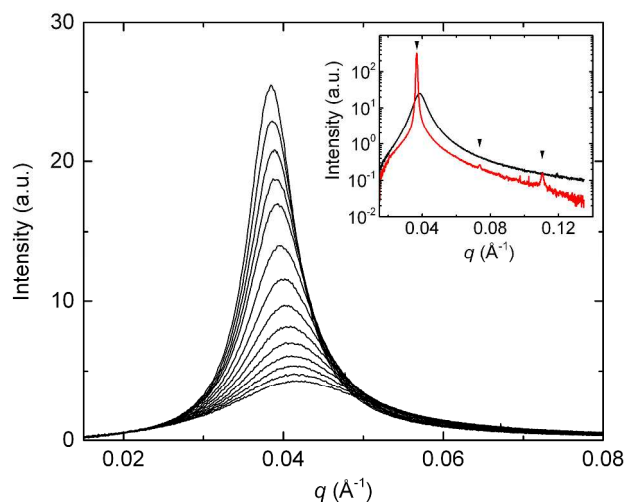


Figure S1. SAXS spectra of the disordered state for PCHE-PE-14 upon heating (190 – 300 °C). The inset plot shows background-subtracted SAXS spectra for an ordered lamellar morphology (red, 140 °C) and a disordered state (black, 190 °C).

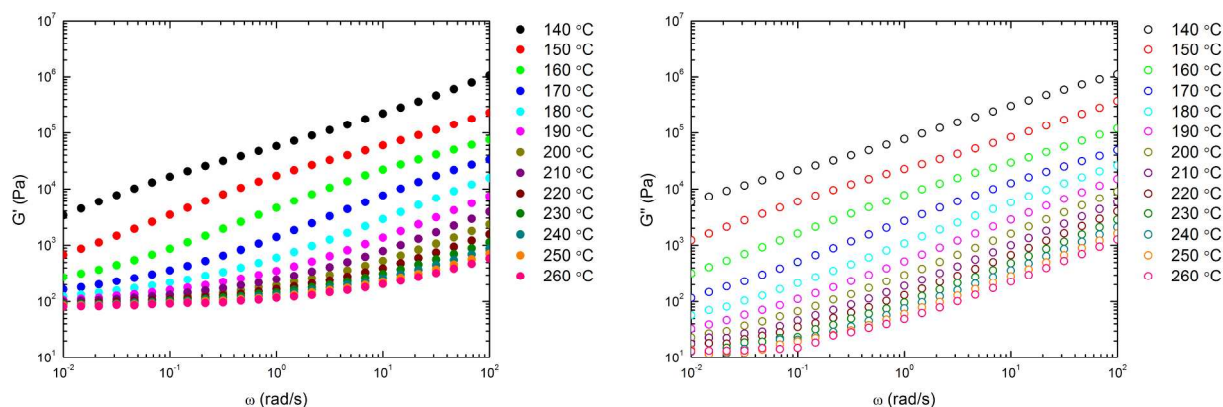


Figure S2. Plots of the dynamic storage (G') and loss (G'') moduli for PCHE-PE-19 (18.9 kg/mol) as a function of ω . Data were obtained from dynamic frequency sweeps at various temperatures and strain % values listed in Table S1. The order-disorder transition for PCHE-PE-19 is 317 ± 1 °C.

Table S1. The strain (%) and shift factors (a_T) used for the time-temperature superposition of PCHE-PE-19.

Temperature (°C)	Strain (%)	a_T
140	0.7	900
150	0.7	110
160	1.0	17
170	1.0	3.5
180	1.0	1
190	1.0	0.35
200	1.0	0.14
210	1.0	0.065
220	1.0	0.04
230	1.0	0.025
240	1.0	0.015
250	1.0	0.01
260	1.0	0.009

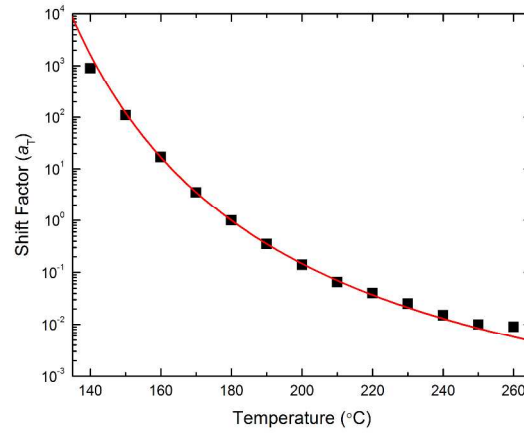


Figure S3. Shift factors (a_T) for PCHE-PE-19 as a function of temperature.

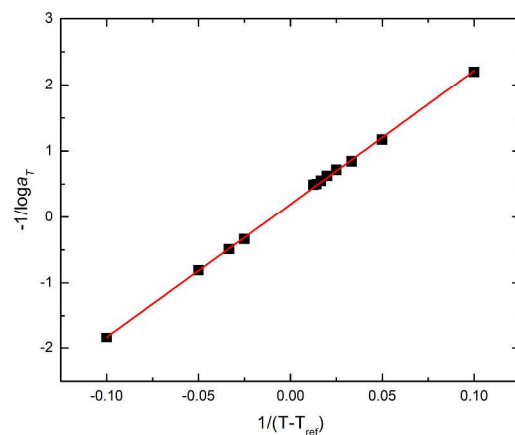


Figure S4. Linear WLF fit for PCHE-PE-19. The reference temperature is 180 °C. The WLF parameters were calculated to be $c_1 = 5.16$ and $c_2 = 104.25$ °C, with a reference temperature of 180 °C.

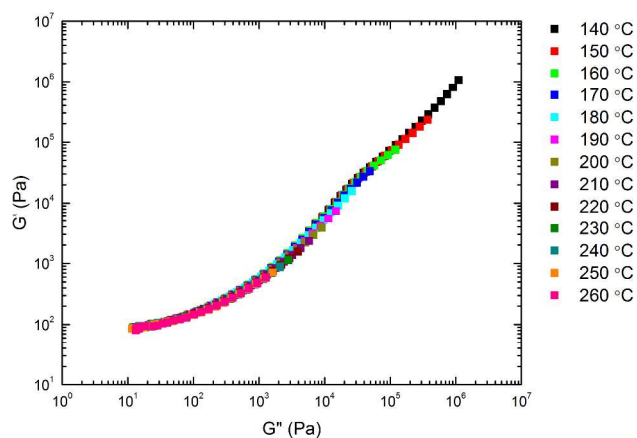


Figure S5. Cole-Cole plot of PCHE-PE-19 (18.9 kg/mol).

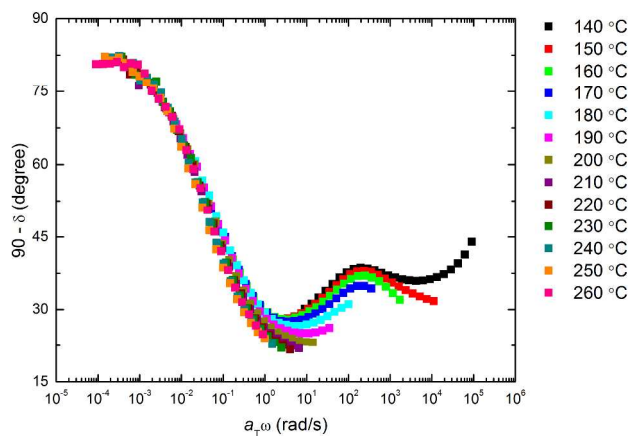


Figure S6. Phase angle versus shifted frequency for PCHE-PE-19. Shift factors (a_T) were applied to the frequency with a reference temperature of 180 °C and $c_1 = 5.16$ and $c_2 = 104.25$ °C.

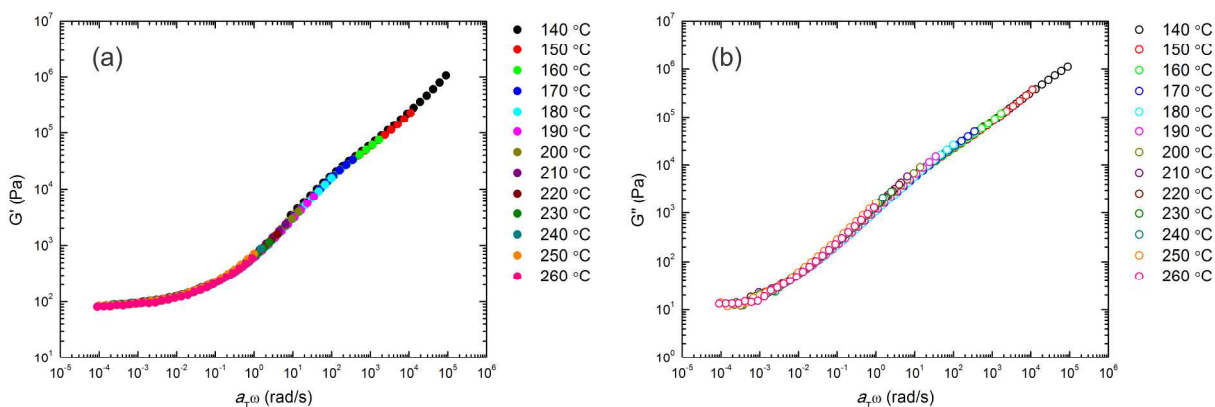


Figure S7. The tTS master curve for the (a) dynamic storage (G') and (b) loss (G'') moduli for PCHE-PE-19. Shift factors (a_T) were applied to the frequency with a reference temperature of 180 °C and $c_1 = 5.16$ and $c_2 = 104.25$ °C

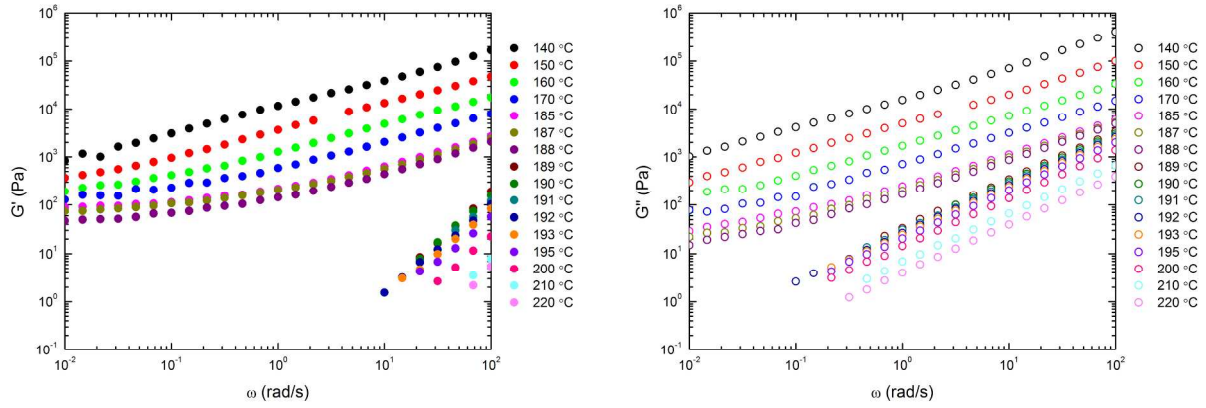


Figure S8. Plots of the dynamic storage (G') and loss (G'') moduli as a function of ω for PCHE-PE-14 near the order-disorder transition (189 ± 1 °C). The data was obtained from dynamic frequency sweeps at the various isothermal temperatures and strain % listed in Table S2.

Table S2. Strain (%) and shift factors (a_T) used for the time-temperature superposition of PCHE-PE-14. The applied a_T values used were calculated from the WLF equation, as determined from PCHE-PE-19, with a reference temperature of 180 °C and $c_1 = 5.16$ and $c_2 = 104.25$ °C.

Temperature (°C)	Strain (%)	a_T
140	0.05	900
150	0.05	110
160	0.05	17
170	0.05	3.5
180	0.1	1
185	0.5	0.58
187	0.5	0.47
188	0.5	0.43
189	0.5	0.39
190	1.0	0.35
191	1.0	0.32
192	3.0	0.29
193	3.0	0.27
195	3.0	0.22
200	3.0	0.14
210	5.0	0.065
220	15	0.04

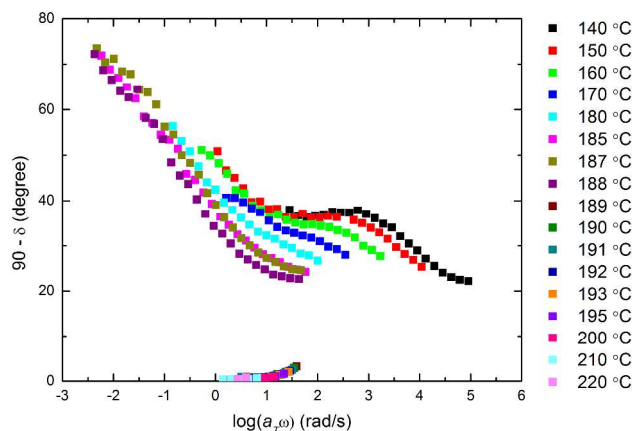


Figure S9. Phase angle versus shifted frequency for PCHE-PE-14. Shift factors (a_T) were applied to the frequency with a reference temperature of 180 °C and $c_1 = 5.16$ and $c_2 = 104.25$ °C.

Example Longest Relaxation Time Calculation

PCHE-PE-14:

In the work presented here, a PCHE homopolymer with $M_n = 7.6$ kg/mol was estimated to have a single-chain relaxation time of 0.03 s at 190 °C. This value was determined from the crossover frequency where $G'(\omega) = G''(\omega)$ in DMS spectra from a previously published report of the viscoelastic properties of PCHE homopolymers.¹ Specifically, the crossover frequency for a $M_n = 13.4$ kg/mol PCHE homopolymer was $a_T\omega \approx 20$ rad/s, which was determined from a master curve described by WLF parameters with values, $c_1 = 8.51$ and $c_2 = 104.3$ °C at a $T_{\text{ref}} = 187$ °C. To calculate the relevant PCHE relaxation time (i.e. for $M_n = 7.6$ kg/mol, $T = 190$ °C), it was necessary to make corrections for differences in T and M_n using reported WLF parameters and the Rouse ($\tau_1 \sim M_n^2$) scaling relationship, respectively. The Rouse ($\tau_1 \sim M_n^2$) scaling relationship was used because both PCHE homopolymers are unentangled. The value of a_T at 190 °C is 0.58, Therefore, the corrected single-chain relaxation time for a PCHE homopolymer with a molecular weight of 13.4 kg/mol and 7.6 kg/mol at 190 °C is 0.03 s and 0.009 s, respectively.

A similar method was used for PE. The experimental single-chain relaxation time for a PE homopolymer with $M_n = 109$ kg/mol was 0.0071 s at 190 °C.² The reptation ($\tau_{\text{rep}} \sim M_n^{3.4}$) scaling relationship was used because both PE homopolymers are entangled.

Table S3. Entanglement molecular weight (M_e), glass transition temperature (T_g), and calculated homopolymer single-chain relaxation times (τ).

Diblock Copolymer	Chain M_w (kg/mol) ^a	M_e (kg/mol) ^b	T_g (°C) ^c	τ	Rheological Fingerprint ^e
PCHE-PE $T = 190$ °C	PCHE (7.6) ¹ PE (6.0) ²	39.0 ¹ 0.8 ³	140 ¹ −120 ⁴	9.3 x 10 ^{−3} 3.7 x 10 ^{−7}	No
PtBS-PMMA $T = 180$ °C	PtBS (8.4) PMMA (9.3)	37.6 ⁵ 10.0 ³	141 ⁶ 110 ⁶	n/a ^d	Yes ⁷
PS-PI $T = 180$ °C	PS (10.7) ⁸ PI (10.3) ¹⁰	13.3 ³ 5.4 ³	100 ⁴ −60 ¹¹	6.7 x 10 ^{−2} 1.8 x 10 ^{−6}	No ⁹
1,2-PBD-1,4-PBD $T = 100$ °C	1,2 PBD (50.4) ¹² 1,4 PBD (30.9) ¹⁵	3.1 ³ 1.8 ³	3 ¹³ −89 ¹³	2.0 x 10 ^{−3} 7.6 x 10 ^{−4}	Yes ¹⁴
PEP-PEE $T = 96$ °C	PEP (28.0) ¹⁶ PEE (22.0) ¹⁶	2.3 ³ 11.0 ³	−56 ¹¹ −20 ¹¹	3.6 x 10 ^{−4} 8.4 x 10 ^{−5}	Yes ¹⁶

(a) References indicate where longest relaxation times were determined for the respective homopolymers. (b) References indicate publications where M_e was reported. (c) References indicate publications where T_g was reported. (d) Reported homopolymer relaxation spectra for PtBS and PMMA were for highly entangled systems, therefore, single-chain relaxation times were not estimated for the unentangled blocks of the PtBS-PMMA-236 system. Instead, the ratio τ was assumed to be approximately 1 since both blocks are unentangled and exhibit an identical T_g . (e) References indicate publications where diblock copolymer rheology exhibited the rheological fingerprint.

Example ΔT_g Correction of Longest Relaxation Time for 1,2-PBD-1,4-PBD

The T_g s for the constituent blocks of 1,2-PBD-1,4-PBD were estimated from differential scanning calorimetry (DSC) measurements reported in Figure 5 in Bates *et al.*¹³ The T_{ODT} of the material of interest for which the rheological fingerprint of fluctuations is reported (BB6) is well above the measured constituent block T_g s. Since the block T_g s are known to depend on the state of segregation in a block polymer, we used the DSC trace of a different sample (BB2) to estimate the T_g s of the constituent blocks under thermodynamic conditions which most closely approximate those where the rheological fingerprint of fluctuations was measured in BB6 (i.e. in the fluctuating disordered phase near T_{ODT}). Sample BB2 was chosen since it is in the fluctuating

disordered phase when the material vitrifies.¹⁴ T_g s of the 1,2-PBD and 1,4-PBD blocks were estimated to be -30 and -75 °C, respectively.

To incorporate the estimated block T_g s into our calculation of the block relaxation times outlined above, we took advantage of the fact that WLF parameters are nearly universal when $T_{\text{ref}} = T_g$. We converted reported 1,2-PBD and 1,4-PBD WLF parameters to have $T_{\text{ref}} = T_g$ of the homopolymers (3 and -89 °C, respectively). These WLF parameters were then used to calculate shift factors using the estimated T_g s of the 1,2-PBD and 1,4-PBD blocks in BB6 (-30 and -75 °C, respectively) as T_{ref} . This procedure results in longest relaxation times of 3.8×10^{-4} s and 1.1×10^{-4} s for the 1,2-PBD and 1,4-PBD blocks, respectively, and $\tau_r = 3$.

REFERENCES

1. Zhao, J.; Hahn, S. F.; Hucul, D. A.; Meunier, D. M. *Macromolecules* **2001**, *34*, 1737-1741.
2. Vega, J. F.; Aguilar, M.; Martínez-Salazar, J. J. *Rheol.* **2003**, *47*, 1505-1521.
3. Fetters, L. J.; Lohse, D. J.; Richter, D.; Witten, T. A.; Zirkel, A. *Macromolecules* **1994**, *27*, 4639-4647.
4. Hiemenz, P. C.; Lodge, T. P., *Polymer Chemistry*. 2nd ed.; CRC Press: Boca Raton, FL, 2007.
5. Watanabe, H.; Chen, Q.; Kawasaki, Y.; Matsumiya, Y.; Inoue, T.; Urakawa, O. *Macromolecules* **2011**, *44*, 1570-1584.
6. Kenemur, J. G.; Hillmyer, M. A.; Bates, F. S. *Macromolecules* **2012**, *45*, 7228-7236.
7. Kenemur, J. G.; Hillmyer, M. A.; Bates, F. S. *ACS Macro Lett.* **2013**, *2*, 496-500.
8. Baumgaertel, M.; Schausberger, A.; Winter, H. H. *Rheol Acta* **1990**, *29*, 400-408.
9. Choi, S.; Han, C. D. *Macromolecules* **2004**, *37*, 215-225.
10. Abdel-Goad, M.; Pyckhout-Hintzen, W.; Kahle, S.; Allgaier, J.; Richter, D.; Fetters, L. J. *Macromolecules* **2004**, *37*, 8135-8144.
11. Bates, F. S.; Rosedale, J. H.; Bair, H. E.; Russell, T. P. *Macromolecules* **1989**, *22*, 2557-2564.
12. Roovers, J.; Toporowski, P. M. *Macromolecules* **1992**, *25*, 3454-3461.
13. Bates, F. S.; Bair, H. E.; Hartney, M. A. *Macromolecules* **1984**, *17*, 1987-1993.
14. Bates, F. S. *Macromolecules* **1984**, *17*, 2607-2613.
15. Baurngaertel, M.; De Rosa, M. E.; Machado, J.; Masse, M.; Winter, H. H. *Rheol Acta* **1992**, *31*, 75-82.
16. Rosedale, J. H.; Bates, F. S. *Macromolecules* **1990**, *23*, 2329-2338.